Xu, X.; Wang, W.; Li, Z.; Kratz, K.; Ma, N.; Lendlein, A.:

Surface geometry of poly(ether imide) boosts mouse pluripotent stem cell spontaneous cardiomyogenesis via modulating the embryoid body formation process

In: Clinical Hemorheology and Microcirculation (2016) IOS Press

DOI: 10.3233/CH-168107

Surface geometry of poly(ether imide) boosts mouse pluripotent stem cell spontaneous cardiomyogenesis via modulating embryoid body formation process

Xun Xu[a, b, l], Weiwei Wang[a, l], Zhengdong Li[a, b], Karl Kratz[a, c], Nan Ma[a, b, c, *] and Andreas Lendlein[a, b, c, *]

[a] Institute of Biomaterial Science and Berlin-Brandenburg Center for Regenerative Therapies, Helmholtz-Zentrum Geesthacht, Teltow, Germany

[b] Institute of Chemistry and Biochemistry, Freie Universita¨t Berlin, Berlin, Germany

[c] Helmholtz Virtual Institute - Multifunctional Materials in Medicine, Berlin and Teltow, Teltow, Germany

[l] These authors contributed equally to this work.

* To whom correspondence should be addressed:

Prof. Dr. Nan Ma, Prof. Dr. Andreas Lendlein

Email: nan.ma@hzg.de, andreas.lendlein@hzg.de

Phone: +49 (0)3328 352-450

Fax: +49 (0)3328 352-452

Abstract

The permanent loss of cardiomyocytes may lead to the irreversible damage of myocardium in cardiovascular diseases. The induced pluripotent stem cells (iPSCs) with the capacity of differentiation into a variety of cell types including cardiomyocytes showed high potential for efficient heart regeneration. The iPSCs and iPSC-derived embryoid bodies (EBs) as well as the differentiated cardiomyocytes are highly sensitive to the biophysical cues of their microenvironment, and accordingly their behavior and function can be largely modulated by microstructure of the cell culture surface. In this study, we investigated the regulatory effect of microscale roughness on both cardiomyogenesis and secretion of EBs using poly(ether imide) (PEI) cell culture inserts with different levels of bottom roughness (R0: flat surface; R1: rough surface, R_q ~ 4 μm; R2: rough surface, R_q ~ 23 μm). The proliferation rate and cardiomyogenesis of EBs increased with the increase of surface roughness. The EB secretome derived from R2 surface remarkably enhanced the *in vitro* new vessel formation of endothelial cells, as compared to those from R0 and R1. These findings highlight the potential to improve the iPSC/EB-based restoration of cardiovascular function via microstructured biomaterials.

Key words: microroughness, induced pluripotent stem cells, embryoid body, cardiomyogenesis, secretome

1 Introduction

Cardiovascular disease as a critical public health concern remains the number one cause of death globally and the mortality is still growing [63]. Loss or dysfunction of cardiomyocytes caused by myocardial infarction, hypertrophy and ischemia is one of the major parts leading to such a high fatality rate [2, 24]. Despite the ability of a certain level of endogenous regeneration of adult human heart, the function of the irreversibly damaged heart cannot be completely restored due to the insufficiency of functional cardiomyocytes [5, 40]. Some progenitor or adult stem cells including the skeletal myoblasts [35, 43, 60], hematopoietic stem cells [46] and mesenchymal stem cells [34, 54, 61] have been reported to own the capacity of differentiating into cardiomyocyte-like cells either in culture conditions or following intracardiac transplantation, showing potential as therapeutic cell sources in heart regeneration. However, this issue remains controversial so far, as many of them might have limited or even no cardiomyogenic potential [29, 51]. Therefore, to achieve the successful heart regeneration there is an urgent need to find out a promising cell source, which should have a high cardiomyogenic differentiation capacity allowing for getting a large scale of functional cardiomyocytes for transplantation.

The successful generation of induced pluripotent stem cells (iPSCs) by introducing transcription factors opened a new field of stem cell-based regenerative therapy [59]. The iPSCs have become the most promising cell source due to their capability of differentiating into all cell types from three primary germ layers [15, 22] and the

avoidance of ethical concerns. The differentiation of pluripotent stem cells towards the cardiomyocyte linage was first demonstrated in 2000 by generating functional beating cardiomyocytes via the mouse ESC-derived embryoid bodies (EBs) [11]. After that, this technique was widely applied and the cardiomyogenic differentiation potential was subsequently proved in other human pluripotent stem cells [25, 26, 42]. Excitingly, the structure and function of cardiomyocytes derived from pluripotent stem cells were comparable to the isolated neonatal myocadium [20, 36] indicating that pluripotent stem cells could serve as the ideal cell source for cardiac regeneration.

The precisely controlled differentiation process is of great importance for clinical benefits of iPSC-based treatment as well as the avoidance of tumorigenesis [21]. More and more studies have revealed that physical cues could markedly modulate the function and fate of stem cells and EBs [31, 57, 64], besides the chemical cues. In addition, it was found that the cardiomyocyte growth, development, behavior and function could also be modulated by topography [41, 66] of the culture substrates or mechanical cues [9, 38, 55]. However, the knowledge on how the topographic cues affect the cardiomyogenic differentiation process of EBs is still scarce. In this context, we hypothesized here that microscale roughness of cell culture surface could effectively regulate the cardiomyogenesis of iPSC-derived EBs. A series of cell culture inserts with different roughness levels on the bottom was designed and fabricated with poly(ether imide) (PEI), a widely used and commercially available biocompatible polymer with tailoring properties for hematological researches [6, 28, 30, 62], with the consideration that the size of single mouse iPSC (miPSC) is

approximately 10 μm and the EB diameter is typically 100-200 μm after initial 48-72 hours of culture. The smooth surface R0 was utilized as a control. The R1 surface with a roughness level relevant to EB size (R_q ~ 4 μm) and mean peak spacing below 250 μm was expected to accommodate EBs and allowing paracrine sensing between the cells. The R2 surface -with the highest roughness (R_q ~ 23 μm) and a mean peak spacing larger than the dimension of single initial EBs was expected to separate the EBs by preventing EB fusion. By using such a system, the influence of microscale roughness on proliferation and cardiomyogenic differentiation of EBs could be investigated. Both EB reseeding and non-reseeding methods were applied to investigate the potential effects of microroughness on EB-derived cardiomyogenesis and EB secretomes induced angiogenesis.

2 Materials and methods

The study was performed in accordance with the ethical guidelines of the journal Clinical Hemorheology and Microcirculation [1].

2.1 Fabrication and characterization of microroughness substrates

The poly(ether imide) (PEI) with a number average molecular weight (*M*n) of 18000 g/mol (trade name ULTEM® 1000, General Electric, USA) was used for fabricating cell culture inserts via injection molding [52]. Three differently structured cylinders were utilized to create the different bottom roughness: a cylinder with a polished contact surface (R0), and two cylinders with micro-structured surfaces according to the standard of German Institute for Standardization (DIN 16747: 1981-05), M30 (R1)

and M45 (R2).

The roughness profile of the insert bottom was analyzed with an optical profilometer (MicoProf 200, FRT - Fries Research & Technologie GmbH, Bergisch Gladbach, Germany) equipped with a CWL 300 chromatic white-light sensor. Each analysis was performed on an area of 7 x 7 mm^2 (4000 lines per image, 250 dots per line, 300 Hz). The raw data were corrected for the sample tilt (subtraction of a polynom ^{2nd} order) and bulginess (subtraction of a polynom ^{3rd} order), treated with a median filter as well as by discrimination of invalid data. The inserts were sterilized via steam sterilization (121^{o}C, 200 kPa, 20 minutes) using a Systec Autoclave D-65 (Systec GmbH, Germany) prior to biological tests.

2.2 miPSC culture

The miPSCs (male mouse cell line iPS-MEF-Ng-492B-4) was purchased from CiRA, Kyoto University, Japan. This cell line was reprogrammed from mouse embryonic fibroblasts of Nanog-GFP-IRES-Puro^{r} transgenic mice without integration of exogene transfection [45]. The initial culture of miPSCs was performed using mitomycin C treated feeder cells and 0.1% (w/v) gelatin-coated tissue culture dish. The cells were then adapted to xeno- and feeder-free conditions by culturing on 10 µg/ cm^2 of Cultrex mouse laminin I (Bio-Techne GmbH, Germany) coated tissue culture treated plate (TCP) in ESGRO-2i medium (Merck Chemicals GmbH, Germany). The medium was daily changed and the cells from passages 10 to 20 were used for all experiments.

2.3 EB formation and proliferation assay

At day 0, the miPSCs were harvested and seeded with a density of 1×10^4 cells/ cm^2 into PEI inserts and incubated with complete KnockOut serum replacement EB medium (1x DMEM/ F12, 2 mM GlutaMAX-I, 20% KnockOut SR, 0.1 mM non-essential amino acids and 0.1 mM β-mercaptoethanol; Thermo Fisher Scientific, Germany). The EB medium was changed every two days. The EB formation was monitored with a phase-contrast microscope and a confocal laser scanning microscope (LSM 780, Carl Zeiss, Germany). The spontaneous cardiomygenic differentiation of EBs was investigated by continuously culturing EBs in PEI insert (CC-EBs) and reseeding EBs into gelatin (0.1% w/v) coated 48-well TCP on day 3 (RS-EBs). For RS-EBs, at day 3, the EBs harvested from microroughness substrates with the diameters between 100-300 μm were acquired by using strainers with 100 and 300 μm mesh sizes. The number of cells in EBs was determined using a Cell Counting Kit-8 (CCK-8, Dojindo Molecular Technologies, Germany) to evaluate the EB proliferation. Briefly, the EB culture medium was replaced by 300 μL of fresh medium, followed by adding 30 μL of CCK-8 solution per insert/well. After 2.5 hours of incubation at 37 °C, 100 μL medium/ CCK-8 mixture was transferred into a transparent flat bottom 96-well TCP from each insert or well, and the absorbance of the mixture was measured at a wavelength 450 nm and a reference wavelength 650 nm using a microplate reader (Infinite 200 PRO, Tecan Group Ltd., Switzerland). The relative cell number was calculated via a standard curve, which was produced by measuring a series of samples with known cell number.

2.4 Conditioned media collection and tube formation

The tube formation of human hmbilical vein endothelial cells (HUVECs) was tested using the EB conditioned media (CM). The medium was collected at day 3 and day 10 from CC-EBs and RS-EBs, respectively. The total protein amount in the CM was quantified using a BCA protein assay kit (Thermo Fisher Scientific, Germany). Then, the CM was adjusted to contain the same amount of total proteins by diluting with the KnockOut serum replacement EB medium. To assess the new vessel formation potential of HUVECs, the 96-well TCP was firstly coated with 100 μL/ cm^2 Geltrex solution (Thermo Fisher Scientific, Germany). Then, HUVEC cells were seeded with a density of 4.5×10^4 cells/ cm^2. For each well, 100 μL of diluted CM containing 50 μg total protein was applied for cell culture. The tube formation of HUVEC cells was observed with a phase contrast microscope. The images were taken in randomly selected observation fields and the tube elements were quantified by ImageJ software with the angiogenesis analyzer plugin. The segments, nodes/ junctions, branches, tubes and meshes were recognized and quantified by the software. The segments and junctions, which connected with each other to form the complete loops, were defined as the master segments and junctions.

2.5 Alkaline phosphatase and immunohistochemistry staining

An alkaline phosphatase (AP) staining kit (Miltenyi Biotec, Germany) was applied for staining of undifferentiated miPSCs. The cells were washed with phosphate buffered saline with tween-20 and fixed at room temperature for 5 min. After washing, freshly

prepared AP substrate was added and the cells were incubated in dark at room temperature. The reaction was stopped when purple stain of cells was appeared. The cardiomyocyte characterization kit (Merck Chemicals GmbH, Germany) was used to visualize the specific markers of EB-derived cardiomyocytes. Cells were fixed, permeabilized and blocked using Image-iT fixation/ permeabilization kit (Thermo Fisher Scientific, Germany) according to the user manual. Cells were then stained with primary antibodies (sheep anti-Tropomyosin and mouse anti-Troponin I) overnight at 4 °C and the corresponding Alexa Fluor 488 or 633 conjugated anti-sheep or mouse IgG (H+L) secondary antibodies (Thermo Fisher Scientific, Germany) for 1h at room temperature in dark. Hoechst 33342 (Thermo Fisher Scientific, Germany) was applied for nuclei staining. The IX81 motorized inverted fluorescent microscope (Olympus, Germany) was used for imaging.

2.6 Time-lapse microscopy

The EB formation of miPSCs (day 1 ~ day 3) and the beating of the spontaneously differentiated EBs (day 8 for CC-EBs and day 12 for RS-EBs) were tracked using a phase contrast time-lapse imaging microscope (IX81 motorized inverted microscope, Olympus, Germany) equipped with a bold line cage incubator providing the humidified atmosphere (37 °C, 5% CO_2). miPSCs were added into the inserts at a density of 3×10^4 cells/ cm^2. Cells cultured on R1 and R2 were monitored from day 1 until day 3 after cell seeding to monitor the aggregation and migration of the semi-attached cells or EBs. The beating of the cardiomyogenic differentiated EBs was

tracked for 8 seconds. The total beating cycles for each video was counted manually afterwards.

2.7 Flow cytometry

Before seeding the cells into PEI inserts, the cells were characterized using a human and mouse pluripotent stem cell analysis kit (Stemflow, BD Biosciences, Germany). The surface markers SSEA1 and SSEA4 were firstly stained by using mouse anti-SSEA1-PE and mouse anti-SSEA4-Alexa Fluor 647 monoclonal antibodies provided in the kit. Cells were than washed, fixed and permeabilized. Subsequently, cells were immunostained by mouse anti-Oct4-PerCP-Cy 5.5 for 30 min in dark at room temperature. The isotype control antibodies in the kit were used in parallel. Then, the cells were analyzed via flow cytometry and the data was processed with Flowjo software (Tree Star Inc., USA). To analyze the cell cycle kinetics alteration, the miPSCs were seeded into the inserts with the density of 1×10^4 cells/ cm^2. After 3 days of culture, the formed EBs were treated with Accumax (Merck Chemicals GmbH, Germany) to obtain single cells. Then, the cells were fixed overnight with cold 70% ethanol, and subsequently stained with FxCycle™ PI/RNase staining solution (Thermo Fisher Scientific, Germany) at room temperature for 30 min. The cell cycle was determined using flow cytometry, and the fractions of cells in different phases were analyzed using ModFit LT software (Verity Software House, USA).

2.8 Statistics

Statistical analysis was performed using the two-tailed unpaired independent-samples

t- test, and a p value less than 0.05 was considered to be significant. Data are presented as mean ± standard deviation (SD) unless stated otherwise.

3 Results

3.1 Poly(ether imide) substrates with different microroughness

To study the influence of the microroughness on the EB formation and spontaneous cardiomyogenesis, the PEI cell culture insert was designed with a suitable size to fit the standard 24-well TCP (18 mm height, 11 mm inner and 13 mm outer diameter of the bottom) and the inserts with different types of bottom roughness were prepared via injection molding (Fig. 1A). The surface profile of the PEI insert bottom surface with microroughness was measured by optical profilometry. The root mean square roughnesses (R_q) of the investigated surfaces were 0.2 ± 0.1 µm, 3.9 ± 0.2 µm and 22.7 ± 0.8 µm, respectively, which were named R0, R1 and R2 (Fig. 1B). Two culture strategies were applied in the present strudy. As shown in Fig. 1C, miPSCs were seeded on microrough substrates, at day 3, the formed EBs were either sustained on the same surfaces (CC-EBs) or transferred at the same range of diameters and amounts into a gelatin-coated 48-well TCP (RS-EBs). After additional 5 to 9 days, the cultivation was stopped once the majority of EBs were started to beat (day 8 for CC-EBs and day 12 for RS-EBs).

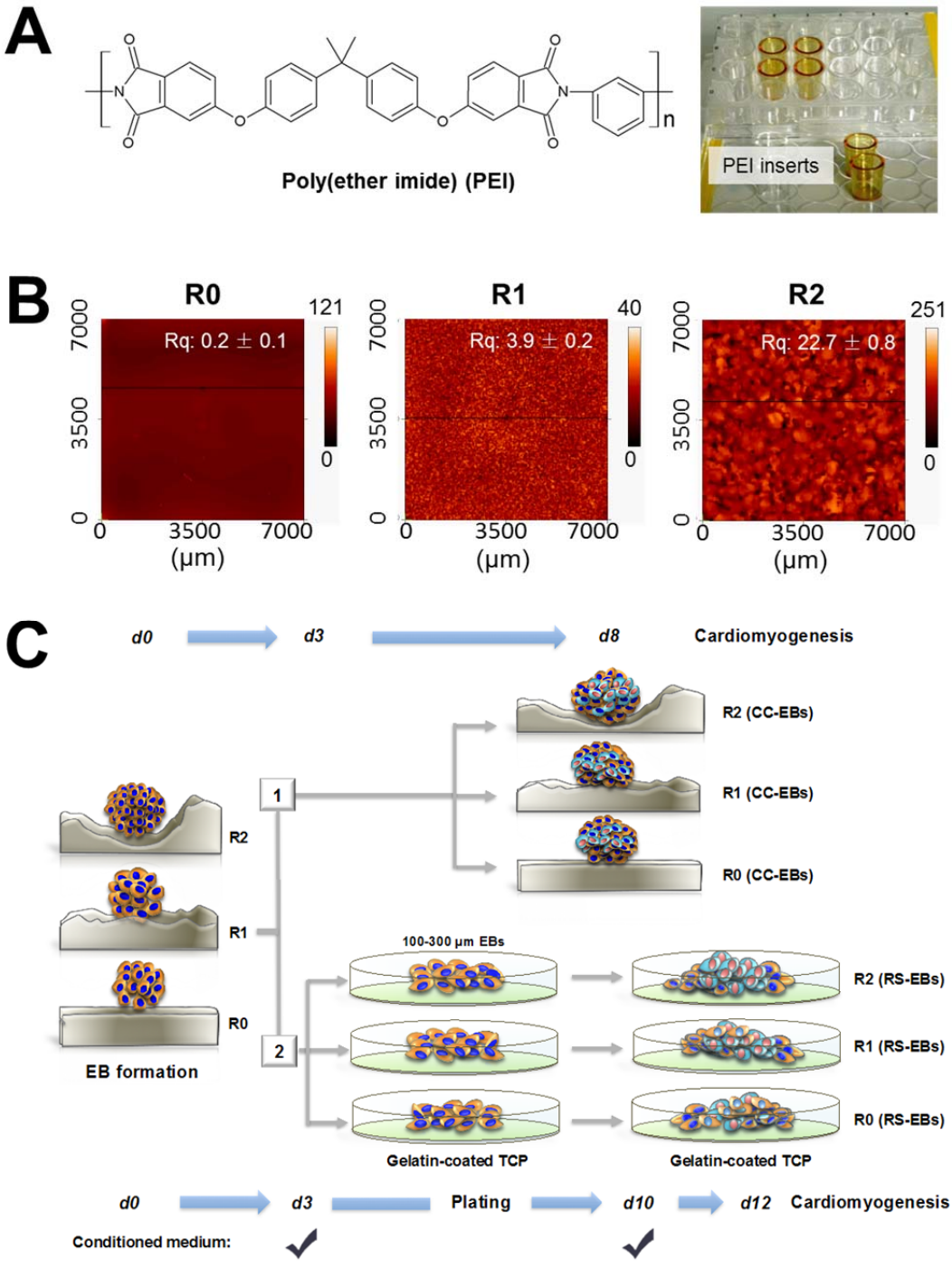

Fig. 1. Design of microroughness cell culture inserts and schematic diagram of EB-based spontaneous cardiomyogenesis. (A) Chemical structure of PEI and image of PEI-based cell culture inserts. (B) Design of the PEI inserts for 24-well TCP with optimal dimensions and the optical profilometry images of the fabricated PEI inserts

comprising three different levels of microroughness. (C) Illustration of two culture strategies for generating EB-derived cardiomyocyte.

3.2 miPSC characterization

After a long-term culture on laminin-coated TCP, miPSCs at passage 20, which had been adapted to the feeder-free and xeno-free culture condition for 10 passages maintained their typical morphology of prominent nucleoli with high nucleo-cytoplasmic ratio and were growing as compact colonies (Fig. 2A, left panel).

To assess the purity and the self-renewal stage of miPSCs for subsequently EB formation and cardiomyogenesis, it is necessary to evaluate the levels of the surface and nuclear stemness markers. As expected, the stemness markers were preserved in the miPSCs at passage 20 via AP staining (Fig. 2A, right panel) and intracellular flow cytometry analysis. Approximately 90% of cells were positive for SSEA1and Oct4, and negative for SSEA4 (Fig. 2B).

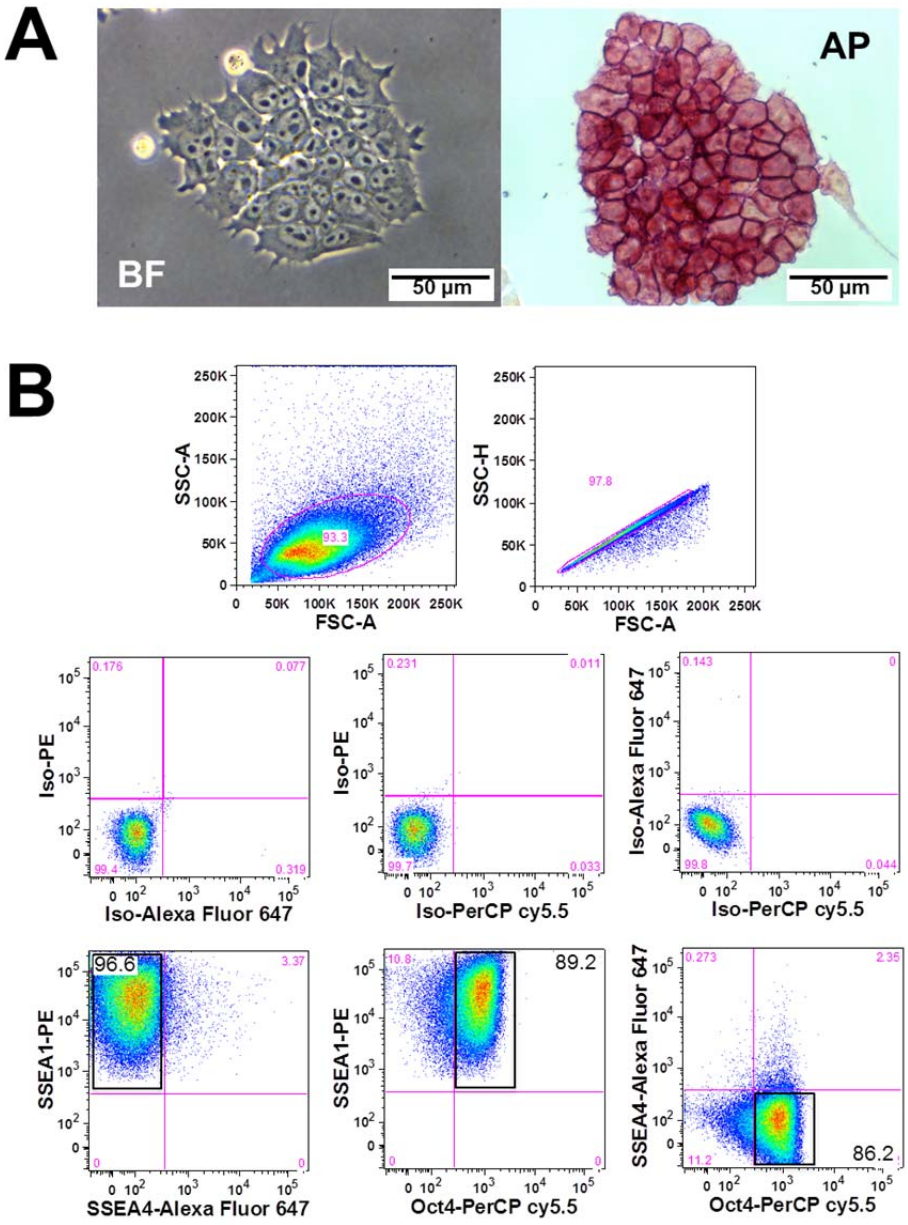

Fig. 2. Characterization of miPSCs at passage 20. (A) miPSCs were adapted and cultured under the xeno-free and feeder-free condition, showing typical colony morphology (left panel) and positive expression of alkaline phosphatase (right panel) (bar = 50 µm). (B) The cells presented positive surface marker SSEA1 and nuclear transcription factor Oct4 according to flow cytometry analysis.

3.3 EB formation and proliferation of EBs

At the initial phase of both continuous and reseeding methods for cardiomyogenesis, as the scheme showed in Fig. 1C, the single cell of miPSCs was seeded on all of the microroughness PEI substrates for three days allowing maturation of EBs. The miPSCs were settled, semi-adherent on PEI surfaces, and rapidly formed tiny cell aggregates especially at the valley area of the R1 and R2 rough surfaces within several hours post seeding (Supplementary video 1 and 2). The small aggregates could merge together or migrate to collect more cells and clusters and became larger and larger to form the 3D spheres with diameters in the range of 200-300 μm (Fig. 3A, left panel; Supplementary video 1 and 2).

The undifferentiated cells during EB formation were monitored via confocal laser scanning microscopy by detection of Nanog-GFP reporter signal. On day 1, although aggregates with a diameter of 100 μm existed, most of the cells kept the stemness and presented the strong GFP signals. Two days later, the EBs were getting larger and larger. On R2 surface, the EBs were growing separately while some of the EBs on other surfaces merged together (indicated by asterisk). A remarkable vanishing of the GFP signal from the inner area of the sphere was observed, which indicated that the cells started to go across the main gateway of the differentiation stage. A slightly increased EB size on R2 surface was observed as compared to those on R0 and R1 surface (Fig. 3A, right panel).

Since the surface structure, particularly the valley area collectively condensed the

miPSCs and efficiently supporting the EB formation, the cell cycle progression and the growth rate were accelerated by increasing the microroughness (Fig. 3B - D). As the preventative flow cytometry histogram and their resulting quantification data showed, G0/G1 to S-phase transition was enhanced during three days of EB formation. Cells stayed in proliferating S and G2M phase were increased by approximately 3% (Fig. 3B and C) resulting in the enhancement of cell expansion by microroughness (Fig. 3D).

As shown in the experimental design scheme in Fig. 1C, at day 3, one group of EBs were kept in the same inserts for differentiation and another group of EBs precultured on microroughness PEI substrates were collected separately. Microroughness could enhance the expansion of cells in EBs cultured on PEI substrates (CC-EBs) (Fig. 3D). However, for the group of EBs transferred to gelatin-coated TCP (RS-EBs), from day 1 post reseeding on gelatin-coated TCPs (day 4, reseeding performed on day 3) till the end of the study at day 12, no significant influence remained on cell expansion from previous cultivation on microrough surfaces (Fig. 3E).

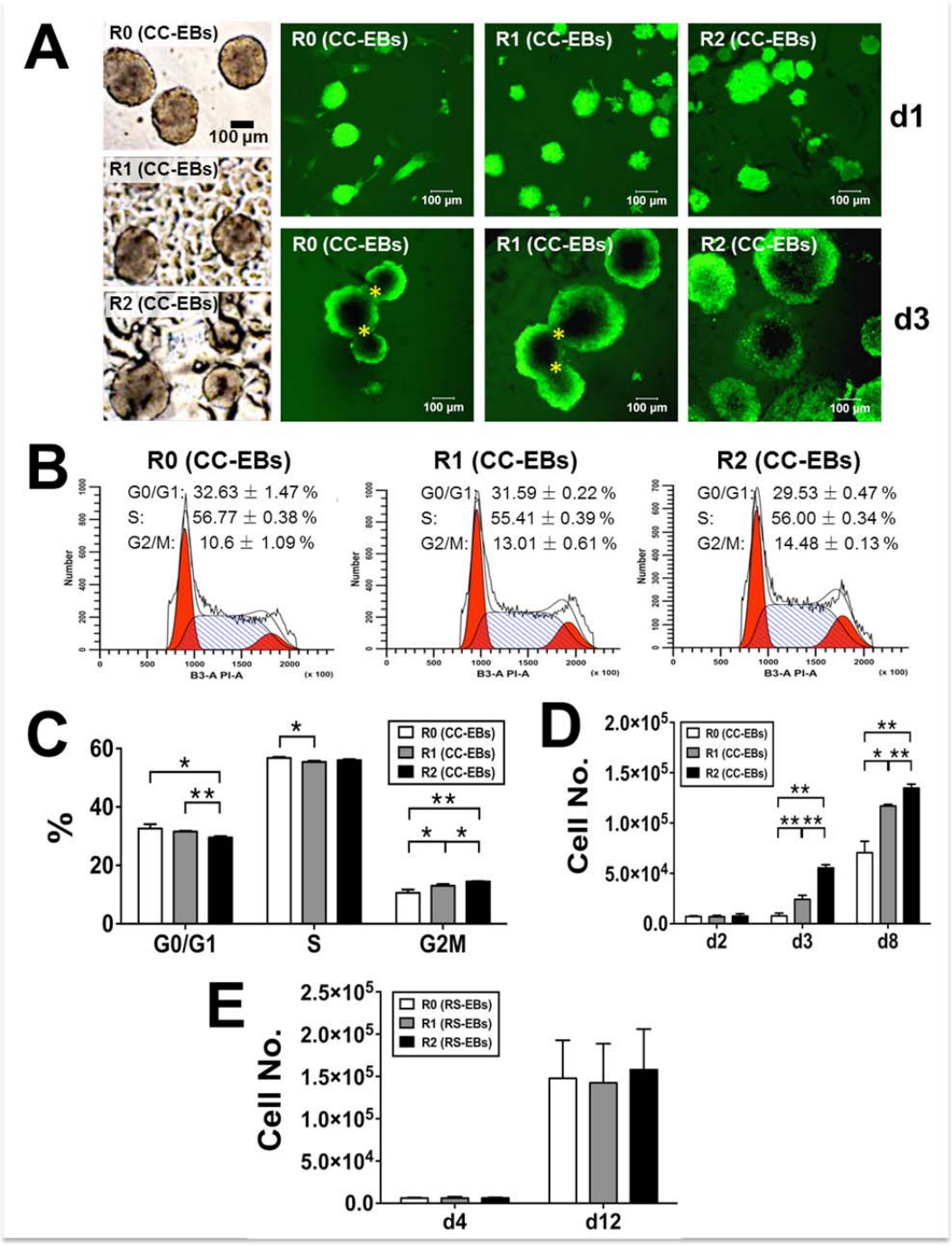

Fig. 3. Characterization of EBs formed from miPSCs. The formed EBs on substrates with different roughness at day 3 (A: left panel). The formation and growth of EBs from Nanog-GFP+ miPSCs was monitored via a confocal laser scanning microscope. The representative images of EBs on different substrates at day 1 and day 3 were shown (A: right panel) (bar = 100 μm), and the merging points of EBs were

pointed out with yellow asterisks. The EBs on different substrates were collected for cell cycle analysis, the representative histograms (B) and the quantitative analysis results (C) were shown. The cell number of EBs at different time points and culture conditions were measured: (D) after 8 days of culture on substrates with different roughness; (E) one day after reseeding on gelatin-coated TCPs (d4, reseeding performed on d3) and the day in which spontaneous beating of cardiomyogenic differentiated cells was observed (d12) (Mean ± SD; n=3; * $p < 0.05$; ** $p < 0.01$).

3.4 Characterization of spontaneous differentiated cardiomyocytes

The CC-EBs directly cultured on microrough surfaces started beating at day 8, the 12-day old RS-EBs adhered and spread on gelatin-coated TCPs also started to contract. From R0 surface, no visible beating was detected from most of the CC-EBs. Notably, beating CC-EBs were mainly located in the valley areas of R1 and R2 microrough surfaces. The spontaneous beating foci from RS-EBs were pointed by yellow asterisks (Fig. 4A).

RS-EBs from gelatin-coated TCPs were immunostained with cardiomyocyte markers Tropomyosin and Troponin I. Larger area of spontaneously differentiated cardiomyocytes in spread EBs and the EB-derived cardiomyocytes with higher volume were found in R2 (RS-EBs) compared to those in R0 (RS-EBs) and R1 (RS-EBs) (Fig. 4B).

To monitor and calculate the rate of beating, spontaneously differentiated and rhythmically contracting EB-derived cardiomyocytes, videos were recorded by

Time-lapse microscope (Supplementary video 3). Compared to the R0 (CC-EBs) and R0 (RS-EBs), almost 3-fold increasing of beating frequency of spontaneously differentiated EBs was detected from the R2 (CC-EBs) (Fig. 4C) and R2 (RS-EBs) (Fig. 4D).

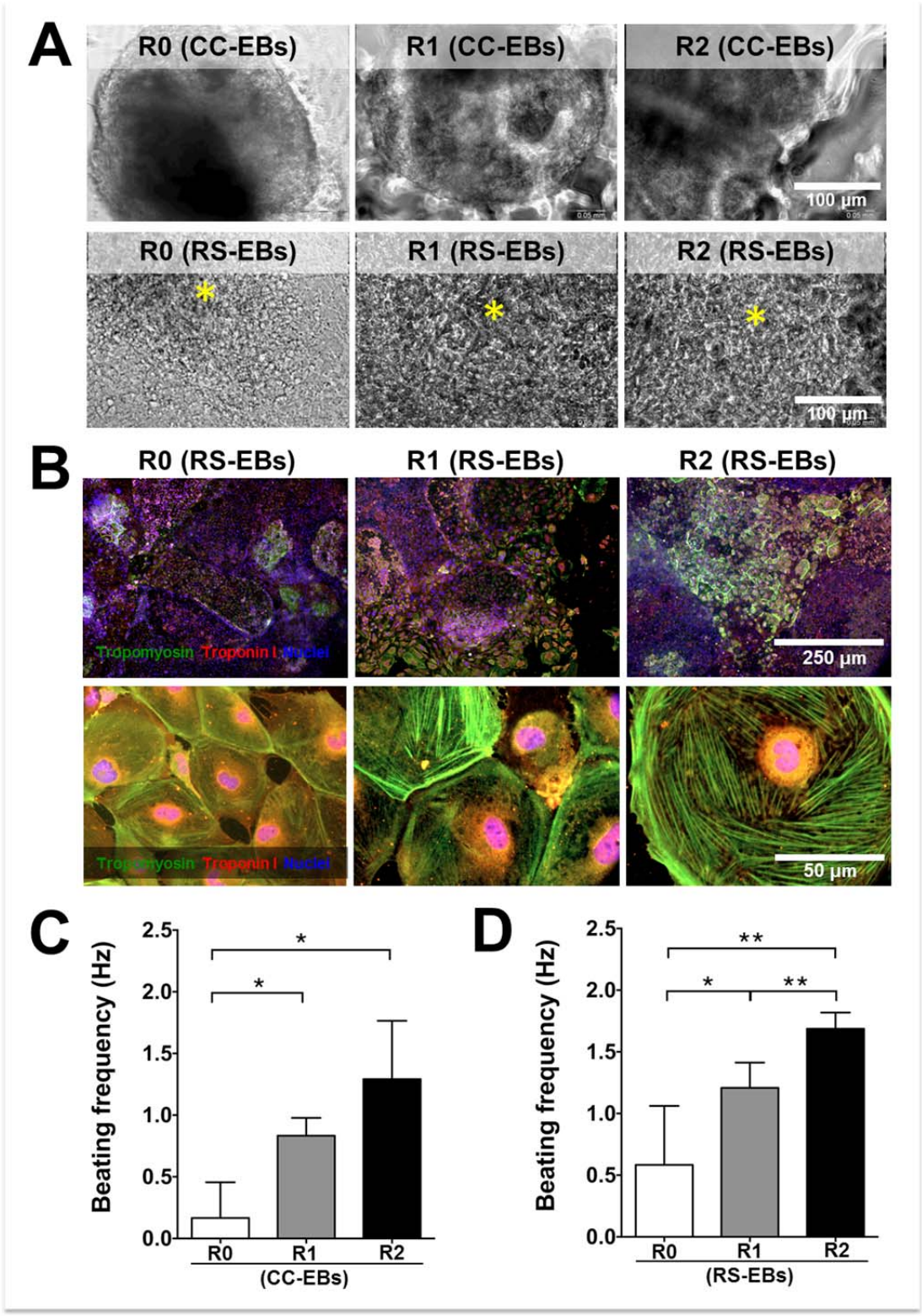

Fig. 4. Characterization of spontaneously differentiated cardiomyocytes from EBs on substrates with different roughness. (A) Representative images of beating and non-beating EBs on **substrates with different roughness (CC-EBs) and**

gelatin-coated TCPs (RS-EBs) (bar = 100 μm). (B) The tropomyosin and troponin I immunostaining of spontaneously differentiated RS-EBs with low and high magnifications (upper panel: bar = 250 μm; lower panel: bar = 50 μm). Quantitative analysis of beating rates of CC-EBs (C) and RS-EBs preconditioned with microrough surfaces (D) (Mean ± SD; C: n=3; D: n=6; * $p < 0.05$; ** $p < 0.01$).

3.5 EB secretomes and new vessel formation

In order to further elucidate whether microroughness not only assisted EB-derived cardiomyogenesis but also benefit for reconstruction of myocardial perfusion system, the CM from EB were adjusted to contain the same amount of proteins and then applied for *in vitro* tube formation of HUVECs.

As shown in Fig. 1C, the CM were collected at day 3 of EB formation and from day 10 EB were transferred and differentiated on gelatin-coated dishes. By overnight incubation with all of the EB CM harvested from different substrates, the orientation of HUVECs plated at subconfluent densities on the Geltrex coated 96-well TCP was reorganized and the cells formed the vessel-like structures simultaneously (Fig. 5A). The constitutive elements of the network such as the segments, branches, junctions and meshes were detected and the numbers as well as the length of the elements were quantified via ImageJ software and the angiogenesis analyzer plugin. The CM derived from EBs cultured on R2 and R2-TCP surface could significantly enhance the *in vitro* new vessel formation of HUVECs compared to accordingly CM from other surfaces (Fig. 5B).

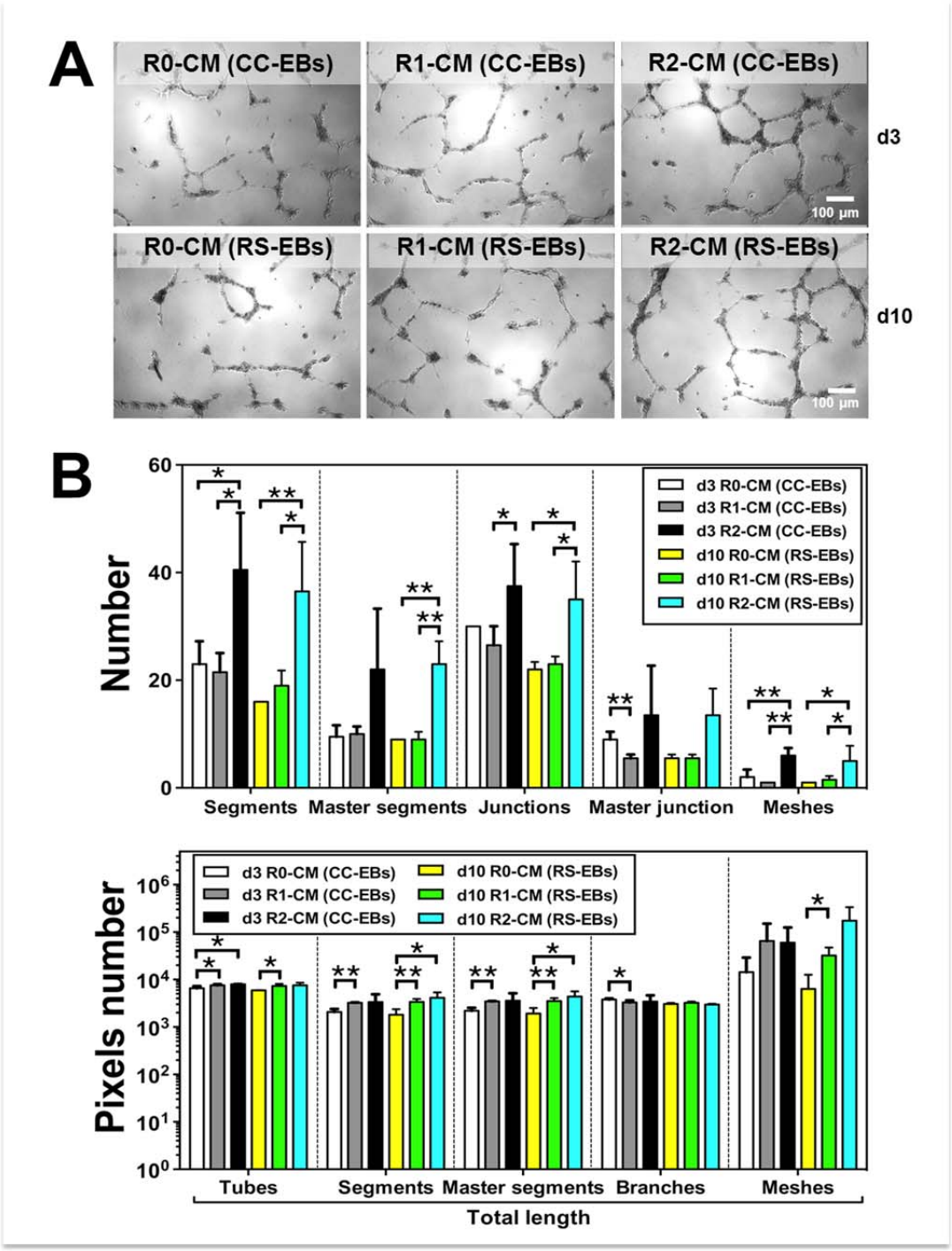

Fig. 5. Tube formation of HUVECs in the presence of EB secretomes derived from microroughness substrates. (A) Phase contrast microscopic images presented the capillary-like structures of the overnight incubated HUVECs growing on Geltrex coated 96-well TCP in the presence of the CM obtained from CC-EBs and RS-EBs

(bar = 100 μm). (B) Image-based quantification was performed by using ImageJ software with the angiogenesis analyzer plugin. The segments, junctions, branches, tubes and meshes were analyzed (Mean ± SD; n=3; * $p < 0.05$; ** $p < 0.01$).

4 Discussion

The pluripotent stem cells proliferate as tight colonies wherein individual cells strongly adhere to each other. When they form EBs, which are defined as 3D pluripotent stem cell aggregates, the cell-cell attachment and communication are particularly critical for determining the behavior and fate of stem cells. Such a biological process is highly dependent on the temporal and spatial arrangement of the cells in EBs. For example, the robust activation of pluripotency associated transcription factor Stat3 and Oct4 could be only observed in mouse pluripotent stem cells with the colony size in the range of 100 to 200 μm [47]. The cell-cell communication via paracrine signaling could be effective only within the limited distance that is around 250 μm [16]. Increasing evidences have suggested that the biophysical property of biomaterials exert an regulatory effect on shape, behavior and differentiation potential of multipotent/pluripotent stem cells and EBs [4, 8, 31, 57, 58, 64], suggesting a promising potential to use biomaterials with defined microstructures or functionalized surface to modulate the pluripotent stem cells or EBs for improved efficacy in stem cell-based regenerative therapy.

It has been reported that the spontaneously and rhythmically contracting cardiomyocytes derived from EBs could be found within several days after plating,

and the number of beating foci as well as the beating rate rapidly increased during differentiation process [19]. Therefore, the EB beating rate was used as a characteristic parameter to define the stage of early cardiomyogenic differentiation as well as the differentiation efficiency. We found that the spontaneous myocardial differentiation of EBs was faster and more efficient on R2 surface than that on the smooth R0 surfaces. Meanwhile, a larger amount of cardiomyocytes derived from EBs were observed on R2 surface as compared to that on R0. These results suggested the improvement of cardiomyogenesis on the surface with appropriate roughness, showing a high potential of culturing EBs on such a surface to fulfill the clinical requirements of large amounts of EBs and differentiated functional myocardiocytes.

EB size has been proved to be important parameters to endogenously regulate cardiomyogenesis of embryonic stem cells [3, 7]. Different approaches and techniques have been adopted to control the EB size and uniformity, including the hanging drop [67], forced-aggregation using microwells [39], microencapsulation [23] and confinement on micropatterns [44, 48], whereby to regulate the differentiation potential of EBs. An improved cardiomyogenic differentiation of EBs has been observed in the hanging drop culture when compared to the conventional suspension culture [67], perhaps due to an enhanced cell-cell contact. The microwells with a diameter of 300 μm allowed the most efficient generation of beating EBs, as compared to the microwells with smaller dimensions [39]. The higher cardiomyogenic differentiation potential of EBs with a diameter of 250–350 μm was also observed after centrifugation in 96-well v bottom plates [7]. Similarly, the

number of contracting EBs was significantly higher on the matrigel patterns with an initial diameter of 400 μm [44]. In our study, by confocal laser scanning microscopy, we only observed a slightly increased EB size on R2 surface, as compared to those on R0 and R1 surface. This might be due to the limited effect of surface roughness on confining the EB size in contrast to the above-mentioned approaches. However, the cell number in EBs on R2 surface was significantly higher than that on R0 and R1 surfaces. This result suggested that in our system the enhanced cardiomyogenesis might be attributed to the higher cell density in EBs, which might lead to the enhanced cell-cell contact and alter the expression of intracellular cardiomyogenic differentiation-associated genes mediated by cell junctions. Further studies are still necessary to clarify this issue.

Previous studies have revealed that the active proliferation contributed not only to the *in vitro* cardiomyogenesis of human embryonic stem cells but also to the in vivo heart development of children and adolescents [10, 40]. Since an increased EB expansion rate was observed on R2 surface, we asked whether the higher cardiomyogenic differentiation of EBs was related to the faster proliferation. Therefore, we performed the experiments by reseeding the EBs on different surfaces into the gelatin coated TCP. After reseeding, all of the EBs presented a similar expansion rate up to 9 days of cultivation, while the cardiomyogenesis was still enhanced for the R2-preconditioned EBs. These observations demonstrated that the cardiomyogenesis of EBs might be not predominantly affected by the EB proliferation rate in our system.

Interestingly, a memory effect [65] was observed in the EBs cultivated on the surfaces with different roughness, in the way that the reseeded EBs presented similar cardiomyogenic potential as those continuously cultured in PEI inserts. We believe that the epigenetic regulation [12], as a potential mechanism to interpret such a phenomenon, might occur at a certain time point and was sustained afterwards to play an important role for memorizing the microroughness promoted cardiomyogenesis. However, further studies focusing on epigenetic aspects, such as histone modification or DNA methylation, should be performed to verify this speculation.

An adequate blood supply and the poor new vessel formation were thought to be the critical issues in cardiovascular regeneration [37]. It has been demonstrated that the clinical benefits from stem cell based therapy was attributed to not only the direct differentiation of stem cells but also the paracrine activity of stem cells. In response to tissue injury, stem cell secretome may exert multiple functions as a cell free therapeutic to stimulate tissue restoration [13, 17, 49]. In our study, the R2 surface showed the potentials of not only improving EB-derived cardiomyogenesis but also stimulating the EB paracrine activity. The significantly enhanced tube formation of HUVEC cells in R2-derived conditioned medium of both CC-EBs and RS-EBs indicated the effectiveness of microscale roughness for regulating stem cell secretome. The design and application of microroughness system for EB-based cardiomyogenesis would be a simple and practical strategy, as both the differentiation and secretion of the EBs could be regulated.

In summary, by using the system comprising PEI surfaces with different microscale roughness and investigating their influence on EBs from miPSCs, we were able to show that the microroughness of culture surface could effectively regulate the proliferation, cardiogenic differentiation and secretion of EBs. Such a regulatory effect was highly dependent on the roughness level, where the R2 surface presented highest effect. The enhanced cardiogenesis of EBs was predominantly due to the cell density in the EBs rather than the EB size and the cell proliferation rate. This might be due to that the closer contact in EBs with higher cell density would activate a series of cardiomyogenic differentiation associated genes. In addition, the observed memory effect suggested that there might be the involvement of epigenetic changes during the culture of cells/EBs on surfaces with microroughness. Concerning the dimensions of the designed PEI substrates, we speculate that the surfaces with microroughness could modulate the cell-cell adhesion and communications via their topographical features. This could contribute to provide the initial growth signals mediated by E-cadherin engagement and the whole complex formation located at the cell-cell adherens junctions [33]. Due to the large plateau area existing between valleys on R2, it might be easier to keep the uniformity of EBs and prevent their fusion. Therefore, on one hand, the roughness structure might offer the three-dimensional space for EB growth; on the other hand, it might be able to maintain the homogeneity of EB and prevent the contact inhibition resulting from EB merging, and consequently regulate a series of signaling pathways such as E-cadherin or Hippo [27]. In this procedure of EB growth and differentiation, in order to transfer the signal from the cell membrane receptors

into the cell nucleus, multiple transmembrane sensors such as integrin [18], E-cadherin [50] and the intracellular messenger proteins [14, 32] are expected to play an important role. Further mechanism studies would be helpful to clarity these issues.

5 Conclusion

The EBs were efficiently formed and the spontaneously beating cardiomyocytes were successfully generated on the PEI substrates with microscale roughness. Our results demonstrated that the microroughness could accelerate EB cell cycle progression, enhance cell proliferation and EB-derived spontaneous cardiomyogenesis. Moreover, the secretome collected from both the continuously cultured cells on surface with microroughness or the rouoghness-preconditioned EBs could promote *in vitro* new vessel formation of endothelial cells. These results highlight the potential of using biomaterials with microstructured surface to regulate iPSCs/EBs, whereby to generate the clinical benefits in stem cell-based cardiovascular system regeneration.

Acknowledgements

The authors acknowledge Mr. Mario Rettschlag for preparation of sterilized PEI inserts, Mrs. Manuela Keller and Mrs. Ruth Hesse for technical support. This work was financially supported by the Helmholtz Association of German Research Centers (including Helmholtz-Portfolio Topic “Technology and Medicine”) and the German Federal Ministry of Education and Research (BMBF project number 0315696A “Poly4Bio BB”).

References

[1] Anonymous, Ethical guidelines for publication in Clinical Hemorheology and Microcirculation: Update 2016, *Clin Hemorheol Microcirc*, **63** (2016), 1-2.

[2] P. Anversa, Myocyte death in the pathological heart, *Circ Res*, **86** (2000), 121-4.

[3] C.L. Bauwens, R. Peerani, S. Niebruegge, K.A. Woodhouse, E. Kumacheva, M. Husain and P.W. Zandstra, Control of human embryonic stem cell colony and aggregate size heterogeneity influences differentiation trajectories, *Stem Cells*, **26** (2008), 2300-10.

[4] C.L. Bauwens, H. Song, N. Thavandiran, M. Ungrin, S. Masse, K. Nanthakumar, C. Seguin and P.W. Zandstra, Geometric control of cardiomyogenic induction in human pluripotent stem cells, *Tissue Eng Part A*, **17** (2011), 1901-9.

[5] O. Bergmann, R.D. Bhardwaj, S. Bernard, S. Zdunek, F. Barnabe-Heider, S. Walsh, J. Zupicich, K. Alkass, B.A. Buchholz, H. Druid, S. Jovinge and J. Frisen, Evidence for cardiomyocyte renewal in humans, *Science*, **324** (2009), 98-102.

[6] S. Braune, M. Lange, K. Richau, K. Lutzow, T. Weigel, F. Jung and A. Lendlein, Interaction of thrombocytes with poly(ether imide): The influence of processing, *Clin Hemorheol Microcirc*, **46** (2010), 239-50.

[7] P.W. Burridge, D. Anderson, H. Priddle, M.D. Barbadillo Munoz, S. Chamberlain, C. Allegrucci, L.E. Young and C. Denning, Improved human embryonic stem cell embryoid body homogeneity and cardiomyocyte differentiation from a novel V-96 plate aggregation system highlights interline variability, *Stem Cells*, **25** (2007), 929-38.

[8] M. Caiazzo, Y. Okawa, A. Ranga, A. Piersigilli, Y. Tabata and M.P. Lutolf, Defined three-dimensional microenvironments boost induction of pluripotency, *Nat Mater*, **15** (2016), 344-52.

[9] C. Chung, B.L. Pruitt and S.C. Heilshorn, Spontaneous cardiomyocyte differentiation of mouse embryoid bodies regulated by hydrogel crosslink density, *Biomater Sci*, **1** (2013), 1082-1090.

[10] L. Cui, K. Johkura, S. Takei, N. Ogiwara and K. Sasaki, Structural differentiation, proliferation, and association of human embryonic stem cell-derived cardiomyocytes in vitro and in their extracardiac tissues, *J Struct Biol*, **158** (2007), 307-17.

[11] P.A. Doevendans, S.W. Kubalak, R.H. An, D.K. Becker, K.R. Chien and R.S. Kass, Differentiation of cardiomyocytes in floating embryoid bodies is comparable to fetal cardiomyocytes, *J Mol Cell Cardiol*, **32** (2000), 839-51.

[12] T.L. Downing, J. Soto, C. Morez, T. Houssin, A. Fritz, F. Yuan, J. Chu, S. Patel, D.V. Schaffer and S. Li, Biophysical regulation of epigenetic state and cell reprogramming, *Nat Mater*, **12** (2013), 1154-62.

[13] D. Drago, C. Cossetti, N. Iraci, E. Gaude, G. Musco, A. Bachi and S. Pluchino, The stem cell secretome and its role in brain repair, *Biochimie*, **95** (2013), 2271-2285.

[14] S. Dupont, L. Morsut, M. Aragona, E. Enzo, S. Giulitti, M. Cordenonsi, F. Zanconato, J. Le Digabel, M. Forcato, S. Bicciato, N. Elvassore and S. Piccolo, Role of YAP/TAZ in mechanotransduction, *Nature*, **474** (2011), 179-83.

[15] M.J. Evans and M.H. Kaufman, Establishment in culture of pluripotential cells from mouse embryos, *Nature*, **292** (1981), 154-6.

[16] K. Francis and B.O. Palsson, Effective intercellular communication distances are determined by the relative time constants for cyto/chemokine secretion and diffusion, *Proc Natl Acad Sci U S A*, **94** (1997), 12258-62.

[17] A. Gazdhar, I. Grad, L. Tamo, M. Gugger, A. Feki and T. Geiser, The secretome of induced pluripotent stem cells reduces lung fibrosis in part by hepatocyte growth factor, *Stem Cell Research & Therapy*, **5** (2014).

[18] Y. Hayashi, M.K. Furue, T. Okamoto, K. Ohnuma, Y. Myoishi, Y. Fukuhara, T. Abe, J.D. Sato, R. Hata and M. Asashima, Integrins regulate mouse embryonic stem cell self-renewal, *Stem Cells*, **25** (2007), 3005-15.

[19] J. Hescheler, B.K. Fleischmann, S. Lentini, V.A. Maltsev, J. Rohwedel, A.M. Wobus and K. Addicks, Embryonic stem cells: a model to study structural and functional properties in cardiomyogenesis, *Cardiovasc Res*, **36** (1997), 149-62.

[20] J. Hescheler, B.K. Fleischmann, M. Wartenberg, W. Bloch, E. Kolossov, G. Ji,

K. Addicks and H. Sauer, Establishment of ionic channels and signalling cascades in the embryonic stem cell-derived primitive endoderm and cardiovascular system, *Cells Tissues Organs*, **165** (1999), 153-64.

[21] S.G. Hong, T. Winkler, C. Wu, V. Guo, S. Pittaluga, A. Nicolae, R.E. Donahue, M.E. Metzger, S.D. Price, N. Uchida, S.A. Kuznetsov, T. Kilts, L. Li, P.G. Robey and C.E. Dunbar, Path to the clinic: assessment of iPSC-based cell therapies in vivo in a nonhuman primate model, *Cell Rep*, **7** (2014), 1298-309.

[22] J. Itskovitz-Eldor, M. Schuldiner, D. Karsenti, A. Eden, O. Yanuka, M. Amit, H. Soreq and N. Benvenisty, Differentiation of human embryonic stem cells into embryoid bodies compromising the three embryonic germ layers, *Mol Med*, **6** (2000), 88-95.

[23] D. Jing, A. Parikh and E.S. Tzanakakis, Cardiac cell generation from encapsulated embryonic stem cells in static and scalable culture systems, *Cell Transplant*, **19** (2010), 1397-412.

[24] J. Kajstura, W. Cheng, K. Reiss, W.A. Clark, E.H. Sonnenblick, S. Krajewski, J.C. Reed, G. Olivetti and P. Anversa, Apoptotic and necrotic myocyte cell deaths are independent contributing variables of infarct size in rats, *Lab Invest*, **74** (1996), 86-107.

[25] S.J. Kattman, A.D. Witty, M. Gagliardi, N.C. Dubois, M. Niapour, A. Hotta, J. Ellis and G. Keller, Stage-specific optimization of activin/nodal and BMP signaling promotes cardiac differentiation of mouse and human pluripotent stem cell lines, *Cell Stem Cell*, **8** (2011), 228-40.

[26] I. Kehat, D. Kenyagin-Karsenti, M. Snir, H. Segev, M. Amit, A. Gepstein, E. Livne, O. Binah, J. Itskovitz-Eldor and L. Gepstein, Human embryonic stem cells can differentiate into myocytes with structural and functional properties of cardiomyocytes, *J Clin Invest*, **108** (2001), 407-14.

[27] N.G. Kim, E. Koh, X. Chen and B.M. Gumbiner, E-cadherin mediates contact inhibition of proliferation through Hippo signaling-pathway components, *Proc Natl Acad Sci U S A*, **108** (2011), 11930-5.

[28] J. Konig, B. Kohl, K. Kratz, F. Jung, A. Lendlein, W. Ertel and G. Schulze-Tanzil, Effect of polystyrene and polyether imide cell culture inserts with different roughness on chondrocyte metabolic activity and gene expression profiles of aggrecan and collagen, *Clin Hemorheol*

Microcirc, **55** (2013), 523-33.

[29] M.A. Laflamme and C.E. Murry, Regenerating the heart, *Nat Biotechnol*, **23** (2005), 845-56.

[30] M. Lange, S. Braune, K. Luetzow, K. Richau, N. Scharnagl, M. Weinhart, A.T. Neffe, F. Jung, R. Haag and A. Lendlein, Surface functionalization of poly(ether imide) membranes with linear, methylated oligoglycerols for reducing thrombogenicity, *Macromol Rapid Commun*, **33** (2012), 1487-92.

[31] D. Li, J. Zhou, F. Chowdhury, J. Cheng, N. Wang and F. Wang, Role of mechanical factors in fate decisions of stem cells, *Regen Med*, **6** (2011), 229-40.

[32] I. Lian, J. Kim, H. Okazawa, J. Zhao, B. Zhao, J. Yu, A. Chinnaiyan, M.A. Israel, L.S. Goldstein, R. Abujarour, S. Ding and K.L. Guan, The role of YAP transcription coactivator in regulating stem cell self-renewal and differentiation, *Genes Dev*, **24** (2010), 1106-18.

[33] W.F. Liu, C.M. Nelson, D.M. Pirone and C.S. Chen, E-cadherin engagement stimulates proliferation via Rac1, *J Cell Biol*, **173** (2006), 431-41.

[34] A.A. Mangi, N. Noiseux, D. Kong, H. He, M. Rezvani, J.S. Ingwall and V.J. Dzau, Mesenchymal stem cells modified with Akt prevent remodeling and restore performance of infarcted hearts, *Nat Med*, **9** (2003), 1195-201.

[35] P. Menasche, A.A. Hagege, J.T. Vilquin, M. Desnos, E. Abergel, B. Pouzet, A. Bel, S. Sarateanu, M. Scorsin, K. Schwartz, P. Bruneval, M. Benbunan, J.P. Marolleau and D. Duboc, Autologous skeletal myoblast transplantation for severe postinfarction left ventricular dysfunction, *J Am Coll Cardiol*, **41** (2003), 1078-83.

[36] J.M. Metzger, L.C. Samuelson, E.M. Rust and M.V. Westfall, Embryonic stem cell cardiogenesis applications for cardiovascular research, *Trends Cardiovasc Med*, **7** (1997), 63-8.

[37] K.C. Michelis, M. Boehm and J.C. Kovacic, New vessel formation in the context of cardiomyocyte regeneration--the role and importance of an adequate perfusing vasculature, *Stem Cell Res*, **13** (2014), 666-82.

[38] A. Mogi, S. Takei, H. Shimizu, H. Miura, D. Tomotsune and K. Sasaki, Effects of Fluid Dynamic Forces Created by Rotary Orbital Suspension Culture on Cardiomyogenic Differentiation of Human Embryonic Stem Cells, *Journal*

of Medical and Biological Engineering, **34** (2013), 101-8.

[39] J.C. Mohr, J. Zhang, S.M. Azarin, A.G. Soerens, J.J. de Pablo, J.A. Thomson, G.E. Lyons, S.P. Palecek and T.J. Kamp, The microwell control of embryoid body size in order to regulate cardiac differentiation of human embryonic stem cells, *Biomaterials*, **31** (2010), 1885-93.

[40] M. Mollova, K. Bersell, S. Walsh, J. Savla, L.T. Das, S.Y. Park, L.E. Silberstein, C.G. Dos Remedios, D. Graham, S. Colan and B. Kuhn, Cardiomyocyte proliferation contributes to heart growth in young humans, *Proc Natl Acad Sci U S A*, **110** (2013), 1446-51.

[41] C. Morez, M. Noseda, M.A. Paiva, E. Belian, M.D. Schneider and M.M. Stevens, Enhanced efficiency of genetic programming toward cardiomyocyte creation through topographical cues, *Biomaterials*, **70** (2015), 94-104.

[42] C.L. Mummery, J. Zhang, E.S. Ng, D.A. Elliott, A.G. Elefanty and T.J. Kamp, Differentiation of human embryonic stem cells and induced pluripotent stem cells to cardiomyocytes: a methods overview, *Circ Res*, **111** (2012), 344-58.

[43] C.E. Murry, R.W. Wiseman, S.M. Schwartz and S.D. Hauschka, Skeletal myoblast transplantation for repair of myocardial necrosis, *J Clin Invest*, **98** (1996), 2512-23.

[44] S. Niebruegge, C.L. Bauwens, R. Peerani, N. Thavandiran, S. Masse, E. Sevaptisidis, K. Nanthakumar, K. Woodhouse, M. Husain, E. Kumacheva and P.W. Zandstra, Generation of human embryonic stem cell-derived mesoderm and cardiac cells using size-specified aggregates in an oxygen-controlled bioreactor, *Biotechnol Bioeng*, **102** (2009), 493-507.

[45] K. Okita, M. Nakagawa, H. Hyenjong, T. Ichisaka and S. Yamanaka, Generation of mouse induced pluripotent stem cells without viral vectors, *Science*, **322** (2008), 949-53.

[46] D. Orlic, J. Kajstura, S. Chimenti, I. Jakoniuk, S.M. Anderson, B. Li, J. Pickel, R. McKay, B. Nadal-Ginard, D.M. Bodine, A. Leri and P. Anversa, Bone marrow cells regenerate infarcted myocardium, *Nature*, **410** (2001), 701-5.

[47] R. Peerani, K. Onishi, A. Mahdavi, E. Kumacheva and P.W. Zandstra, Manipulation of signaling thresholds in "engineered stem cell niches"

identifies design criteria for pluripotent stem cell screens, *PLoS One*, **4** (2009), e6438.

[48] R. Peerani, B.M. Rao, C. Bauwens, T. Yin, G.A. Wood, A. Nagy, E. Kumacheva and P.W. Zandstra, Niche-mediated control of human embryonic stem cell self-renewal and differentiation, *EMBO J*, **26** (2007), 4744-55.

[49] S.H. Ranganath, O. Levy, M.S. Inamdar and J.M. Karp, Harnessing the Mesenchymal Stem Cell Secretome for the Treatment of Cardiovascular Disease, *Cell Stem Cell*, **10** (2012), 244-258.

[50] T. Redmer, S. Diecke, T. Grigoryan, A. Quiroga-Negreira, W. Birchmeier and D. Besser, E-cadherin is crucial for embryonic stem cell pluripotency and can replace OCT4 during somatic cell reprogramming, *EMBO Rep*, **12** (2011), 720-6.

[51] H. Reinecke, E. Minami, W.Z. Zhu and M.A. Laflamme, Cardiogenic differentiation and transdifferentiation of progenitor cells, *Circ Res*, **103** (2008), 1058-71.

[52] T. Roch, A. Kruger, K. Kratz, N. Ma, F. Jung and A. Lendlein, Immunological evaluation of polystyrene and poly(ether imide) cell culture inserts with different roughness, *Clin Hemorheol Microcirc*, **52** (2012), 375-89.

[53] J. Rohwedel, U. Sehlmeyer, J. Shan, A. Meister and A.M. Wobus, Primordial germ cell-derived mouse embryonic germ (EG) cells in vitro resemble undifferentiated stem cells with respect to differentiation capacity and cell cycle distribution, *Cell Biol Int*, **20** (1996), 579-87.

[54] J.G. Shake, P.J. Gruber, W.A. Baumgartner, G. Senechal, J. Meyers, J.M. Redmond, M.F. Pittenger and B.J. Martin, Mesenchymal stem cell implantation in a swine myocardial infarct model: engraftment and functional effects, *Ann Thorac Surg*, **73** (2002), 1919-25; discussion 1926.

[55] S.P. Sheehy, A. Grosberg and K.K. Parker, The contribution of cellular mechanotransduction to cardiomyocyte form and function, *Biomech Model Mechanobiol*, **11** (2012), 1227-39.

[56] I.S. Skerjanc, Cardiac and skeletal muscle development in P19 embryonal carcinoma cells, *Trends Cardiovasc Med*, **9** (1999), 139-43.

[57] S. Sonam, S.R. Sathe, E.K. Yim, M.P. Sheetz and C.T. Lim, Cell contractility arising from topography and shear flow determines human mesenchymal

stem cell fate, *Sci Rep*, **6** (2016), 20415.

[58] Y. Sun, K.M. Yong, L.G. Villa-Diaz, X. Zhang, W. Chen, R. Philson, S. Weng, H. Xu, P.H. Krebsbach and J. Fu, Hippo/YAP-mediated rigidity-dependent motor neuron differentiation of human pluripotent stem cells, *Nat Mater*, **13** (2014), 599-604.

[59] K. Takahashi and S. Yamanaka, Induction of pluripotent stem cells from mouse embryonic and adult fibroblast cultures by defined factors, *Cell*, **126** (2006), 663-76.

[60] D.A. Taylor, B.Z. Atkins, P. Hungspreugs, T.R. Jones, M.C. Reedy, K.A. Hutcheson, D.D. Glower and W.E. Kraus, Regenerating functional myocardium: improved performance after skeletal myoblast transplantation, *Nat Med*, **4** (1998), 929-33.

[61] C. Toma, M.F. Pittenger, K.S. Cahill, B.J. Byrne and P.D. Kessler, Human mesenchymal stem cells differentiate to a cardiomyocyte phenotype in the adult murine heart, *Circulation*, **105** (2002), 93-8.

[62] R. Tzoneva, B. Seifert, W. Albrecht, K. Richau, T. Groth and A. Lendlein, Hemocompatibility of poly(ether imide) membranes functionalized with carboxylic groups, *J Mater Sci Mater Med*, **19** (2008), 3203-10.

[63] M. Writing Group, D. Mozaffarian, E.J. Benjamin, A.S. Go, D.K. Arnett, M.J. Blaha, M. Cushman, S.R. Das, S. de Ferranti, J.P. Despres, H.J. Fullerton, V.J. Howard, M.D. Huffman, C.R. Isasi, M.C. Jimenez, S.E. Judd, B.M. Kissela, J.H. Lichtman, L.D. Lisabeth, S. Liu, R.H. Mackey, D.J. Magid, D.K. McGuire, E.R. Mohler, 3rd, C.S. Moy, P. Muntner, M.E. Mussolino, K. Nasir, R.W. Neumar, G. Nichol, L. Palaniappan, D.K. Pandey, M.J. Reeves, C.J. Rodriguez, W. Rosamond, P.D. Sorlie, J. Stein, A. Towfighi, T.N. Turan, S.S. Virani, D. Woo, R.W. Yeh, M.B. Turner, C. American Heart Association Statistics and S. Stroke Statistics, Heart Disease and Stroke Statistics-2016 Update: A Report From the American Heart Association, *Circulation*, **133** (2016), e38-60.

[64] X. Xu, W. Wang, K. Kratz, L. Fang, Z. Li, A. Kurtz, N. Ma and A. Lendlein, Controlling major cellular processes of human mesenchymal stem cells using microwell structures, *Adv Healthc Mater*, **3** (2014), 1991-2003.

[65] C. Yang, M.W. Tibbitt, L. Basta and K.S. Anseth, Mechanical memory and

dosing influence stem cell fate, *Nat Mater*, **13** (2014), 645-52.

[66] L. Yin, H. Bien and E. Entcheva, Scaffold topography alters intracellular calcium dynamics in cultured cardiomyocyte networks, *Am J Physiol Heart Circ Physiol*, **287** (2004), H1276-85.

[67] B.S. Yoon, S.J. Yoo, J.E. Lee, S. You, H.T. Lee and H.S. Yoon, Enhanced differentiation of human embryonic stem cells into cardiomyocytes by combining hanging drop culture and 5-azacytidine treatment, *Differentiation*, **74** (2006), 149-59.